Temperature evolution of the pseudogap state in the infrared response of underdoped La$_{2-x}$Sr$_x$CuO$_4$

T. Startseva and T. Timusk
Department of Physics and Astronomy, McMaster University, Hamilton, Ontario, Canada L8S 4M1

A. V. Puchkov
Department of Applied Physics, Stanford University, Stanford, California 94305

D. N. Basov
Department of Physics, University of California, San Diego, La Jolla, California 92093

H. A. Mook
Oak Ridge National Laboratory, Oak Ridge, Tennessee 37831

M. Okuya, T. Kimura, and K. Kishio
Department of Applied Chemistry, University of Tokyo, Tokyo 113, Japan
(Received 12 May 1998)

The *ab*-plane optical spectra of two single crystals of underdoped La$_{2-x}$Sr$_x$CuO$_4$ were investigated. The reflectivity of La$_{1.87}$Sr$_{0.13}$CuO$_4$ has been measured in the frequency range 30–9000 cm^{-1} (0.004–1 eV) both parallel and perpendicular to the CuO$_2$ planes, whereas La$_{1.86}$Sr$_{0.14}$CuO$_4$ was studied only in the *ab* plane. The extended Drude model shows that the frequency-dependent effective scattering rate $1/\tau(\omega,T)$ is strongly suppressed below the high-frequency straight-line extrapolation, a signature of the pseudogap state. This suppression can be seen from temperatures below the superconducting transition up to 400 K. In the case of underdoped LSCO the straight-line extrapolation is temperature independent below 200 K, whereas above 200 K there is a strong temperature dependence of the high-frequency $1/\tau(\omega,T)$. The out-of-plane direction is also examined for evidence of the pseudogap state. [S0163-1829(99)08009-1]

The presence of a pseudogap in the normal state of underdoped high-temperature superconductors (HTSC's) is by now widely accepted.[1] The strongest evidence for the pseudogap state comes from recent measurements of angle-resolved photoemission spectra[2] as well as vacuum tunneling.[3] However, these techniques both demand extremely high surface quality and have therefore mainly been restricted to Bi$_2$Sr$_2$CaCu$_2$O$_{8+\delta}$ (Bi221) and YBa$_2$Cu$_3$O$_{7-\delta}$ (Y123) materials, both with two CuO$_2$ layers per unit cell. Techniques that probe deeper into the sample such as dc transport,[4–6] optical conductivity,[7–9] and NMR (Ref. 10) were not only the earliest to show evidence of the pseudogap but have been extended to a much larger variety of materials, including several materials with one CuO$_2$.[6] In all cases evidence for a pseudogap has been reported.

The pseudogap in LSCO as seen by NMR and neutron scattering[11] is rather weak and has led to the suggestion that the existence of the pseudogap in the spin-excitation spectrum is only possible in bilayer compounds such as Y123 and YBa$_2$Cu$_4$O$_4$ (Y124). In particular, Millis and Monien attribute the pseudogap (or the spin gap) to strong antiferromagnetic correlations between the planes in the bilayer, which are responsible for a quantum order-disorder transition.[10]

Apart from having only one CuO$_2$ layer La$_{2-x}$Sr$_x$CuO$_4$ (LSCO) is also a good model system for the study of doping dependences since it can be doped by the addition of strontium over a wide range: from the underdoped, where T_c in-creases with Sr content, to the optimally doped where T_c reaches its maximum value of ≈ 40 K at $x=0.17$, and to the overdoped region where $T_c \rightarrow 0$ at $x=0.34$.[6]

The characteristic signatures of the pseudogap state in the dc resistivity[4] are seen clearly in LSCO.[6,12] These are the striking deviations below a temperature T^* from the high-temperature linear resistivity, resulting in a clear break in slope at T^*. It was found by Batlogg *et al.*[6] that in LSCO T^* decreases from 800 K to approximately 300 K as the doping level is increased from the strongly underdoped to just over the optimal doping level. Similar behavior at $T=T^*$ has been observed in the Hall effect coefficient and the magnetic susceptibility.[13,14]

The pseudogap can also be observed if the conductivity is measured in the frequency domain, $\sigma(\omega)$, where it shows up as a striking depression of the frequency-dependent scattering rate at low frequency. It is found that below a frequency $\Omega_p \approx 600$ cm^{-1}, the scattering rate drops below its high-temperature, high-frequency, linear behavior. This effect has been clearly identified in the bilayer materials.[7–9] One of the aims of this paper is to see if this behavior can also be observed in LSCO. A pseudogap state can be defined in terms of this suppression of scattering: the material is in the pseudogap state when the scattering rate falls below the high-frequency straight-line extrapolation. In the low-frequency limit the scattering rate is proportional to the dc resistivity. Due to this, the $1/\tau(\omega,T)$ suppression should be compared to the suppression of $\rho_{dc}(T)$ (Ref. 6) at tempera-

tures below the linear T dependence region. The IR measurement gives us the possibility to see both the frequency and the temperature dependence of this feature.

A pseudogap feature can also be observed in the *c-axis* IR *conductivity* in the form of a gaplike region of depressed conductivity at low frequency. It has been reported in $YBa_2Cu_3O_{7-x}$ (Y123) and $YBa_2Cu_4O_8$ (Y124) materials[7,15] as well as in LSCO.[16,17] In slightly underdoped LSCO the pseudogap state in the *c-axis* direction is not as well defined as it is in the two-plane materials.[7] However, as the doping is reduced further, the *c-axis* pseudogap state features below 0.1 eV become clearer.[17]

Previous work on the in-plane $\sigma(\omega)$ of the single layer lanthanum strontium cuprate includes work on the oxygen-doped $La_2CuO_{4-\delta}$,[18] thin films of LSCO,[19] as well as work done on a LSCO single crystal at room temperature.[12] To our knowledge, a study of the temperature and doping dependence has not been done. We fill this gap here by performing optical measurements on high-quality LSCO single crystals at temperatures ranging from 10 to 300 K at two different doping levels, both slightly underdoped. Also the optical properties of both the *ab* plane and *c* axis of $La_{1.87}Sr_{0.13}CuO_4$ were measured on the same crystal.

To better display the effect of increased coherence on $\sigma(\omega)_{ab}$ resulting from the formation of the pseudogap state we use the memory function, or extended Drude analysis. In this treatment the complex optical conductivity is modeled by a Drude spectrum with a frequency-dependent scattering rate and an effective electron mass.[20,21] While the optical conductivity tends to emphasize free particle behavior, a study of the frequency dependence of the effective scattering rate puts more weight on displaying the interactions of the free particles with the elementary excitations of the system.[22] The temperature evolution of the frequency-dependent scattering rate and effective mass spectra are of particular interest and are defined as follows:

$$1/\tau(\omega,T) = \frac{\omega_p^2}{4\pi}\text{Re}\left(\frac{1}{\sigma(\omega,T)}\right), \qquad (1)$$

$$\frac{m^*(\omega,T)}{m_e} = \frac{1}{\omega}\frac{\omega_p^2}{4\pi}\text{Im}\left(\frac{1}{\sigma(\omega,T)}\right). \qquad (2)$$

Here, $\sigma(\omega,T) = \sigma_1(\omega,T) + i\sigma_2(\omega,T)$ is the complex optical conductivity and ω_p is the plasma frequency of the charge carriers.

The single crystals of $La_{2-x}Sr_xCuO_4$ with approximate dimensions $5 \times 3 \times 3$ mm^3 were grown by the traveling-solvent floating-zone technique at Oak Ridge[23] in the case of $x=0.14$ and in Tokyo[24] in the case of $x=0.13$. The critical temperature was determined by both superconducting quantum interference device magnetization and resistivity measurements and was found to be 36 K for the nominal concentration of Sr $x=0.14$ and 32 K for $x=0.13$. Since the highest T_c in the LSCO system has been found to be 40 K for $x=0.17$, we conclude that both crystals are underdoped.

The crystal with $x=0.14$ was aligned using Laue diffraction and polished parallel to the CuO$_2$ planes. The crystal with $x=0.13$ was polished in Tokyo to yield both *ab*-plane and *ac*-plane faces. Both surfaces were measured. Polarizers
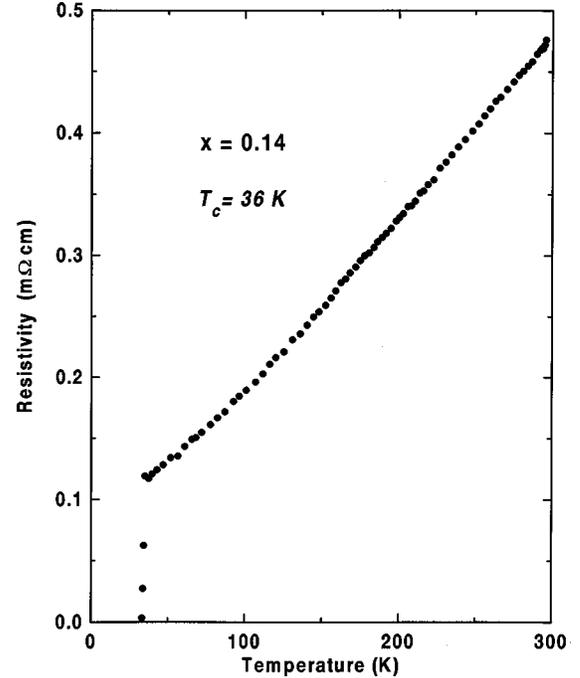

FIG. 1. The temperature dependence of the in-plane resistivity of $La_{1.86}Sr_{0.14}CuO_4$ is shown with a sharp superconducting transition at 36 K. The shape of the curve is consistent with T^* being greater than 300 K.

were used for the *ac*-face data to separate the contribution of CuO$_2$ planes from the *c*-axis optical response.

To get an uncontaminated *ab*-plane measurement, it is important to have the sample surface accurately parallel to the *ab* plane to avoid any *c*-axis contribution to the optical conductivity.[25] The miscut angle between the polished surface normal and the *c* axis was checked by a high precision triple axis x-ray diffractometer and was determined to be less than 0.8%.

All reflectivity measurements were performed with a Michelson interferometer using three different detectors which cover frequencies ranging from 10 to 10000 cm^{-1} (1.25 meV–1.25 eV). The experimental uncertainty in the reflectance data does not exceed 1%. The dc resistivity measurements were carried out using a standard four-probe technique.

The result of the resistivity measurement on the same $La_{1.86}Sr_{0.14}CuO_4$ single crystal used in the optical measurements is shown in Fig. 1. It is commonly accepted that the dc resistivity is linear at high temperatures for LSCO and that the pseudogap begins to form near the temperature where the resistivity drops below this linear trend.[6] At lower temperatures there is a region of superlinear temperature-dependent resistivity. The T^* value for our samples with $x=0.13$ and $x=0.14$ extracted from the phase diagram of Batlogg *et al.*,[6] are 650 and 450 K, respectively. In agreement with this, the resistivity shows a superlinear temperature dependence below room temperature as expected in the pseudogap region.

In Fig. 2 we present the reflectivity data at temperatures above and below T_c for the two samples. For clarity, only three temperatures are shown: $T=300$ K, an intermediate temperature above the superconducting transition and a low temperature ≈ 10 K in the superconducting state. In the fre-

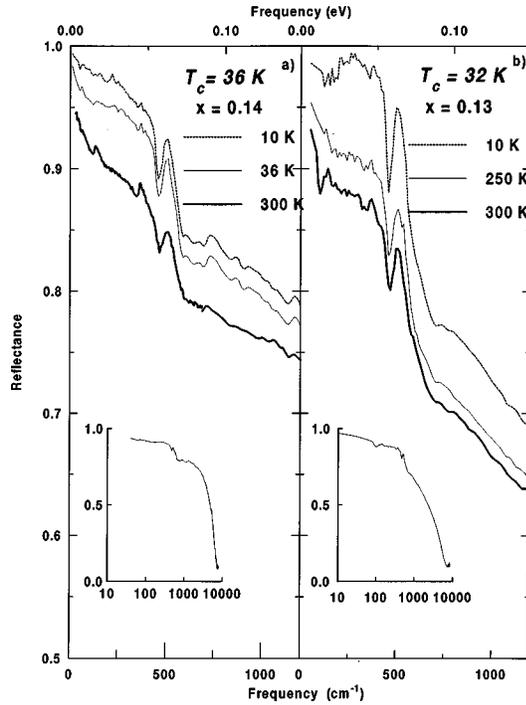FIG. 2. The reflectance of $La_{1.86}Sr_{0.14}CuO_4$ (a) and $La_{1.87}Sr_{0.13}CuO_4$ (b) is shown. The solid lines show normal-state spectra, the dashed curve shows superconducting state spectrum. The thinnest line shows the spectrum at the temperature closest to T_c. The insert in the left panel is a semilog graph of the reflectance at 300 K which shows a plasma edge around 7000 cm^{-1}.

quency region shown the reflectance is strongly temperature dependent for both materials, dropping by approximately 10% as temperature is increased from the lowest temperature to $T = 300$ K. The plasma edge is observed at 7800 cm^{-1} (see inset of Fig. 2). The distinct peaks at approximately 135

and 365 cm^{-1} in the LSCO reflectivity spectra correspond to the excitation of *ab*-plane TO phonons and the peak at 500 cm^{-1} corresponds to a LO phonon.[26] As in all other HTSC materials, the *ab* plane has a coherent response with very high reflectance.

The complex optical conductivity $\sigma(\omega)$ was obtained by Kramers-Kronig analysis of the reflectivity data. Since, in principle, this analysis requires knowledge of the reflectance at all frequencies, reflectivity extensions must be used at high and low frequencies. The Hagen-Rubens formula was used for the low-frequency reflectivity extrapolation, with parameters taken from the dc resistivity measurements on the same sample with $x = 0.14$ shown in Fig. 1 and the results of Takagi *et al.*[27] for the sample with $x = 0.13$. For the high-frequency extension for $\omega > 8000$ cm^{-1} we used the reflectivity results of Uchida *et al.*[12] At frequencies higher than 40 eV the reflectivity was assumed to fall as $1/\omega^4$.

We calculate the plasma frequency of the superconducting charge carriers and the London penetration depth using the following formula:[28]

$$\epsilon_1 = 1 - \frac{\omega_{ps}^2}{\omega^2}. \tag{3}$$

The slope of the low-frequency dielectric function, $\epsilon_1(\omega)$, plotted as a function of w^{-2} in Figs. 3(a) and 3(b) gives plasma frequencies of 6100 and 5700 cm^{-1} in the superconducting state. The corresponding London penetration depths are $\lambda_L = 1/2\pi\omega_{ps} = 250$ nm and 280 nm for $La_{1.86}Sr_{0.14}CuO_4$ and $La_{1.87}Sr_{0.13}CuO_4$, respectively. These values are in good agreement with those obtained previously by Gao *et al.* in films[19] ($\lambda_L = 275 \pm 5$ nm) and by muon-spin-relaxation[29] ($\lambda_L = 250$ nm).
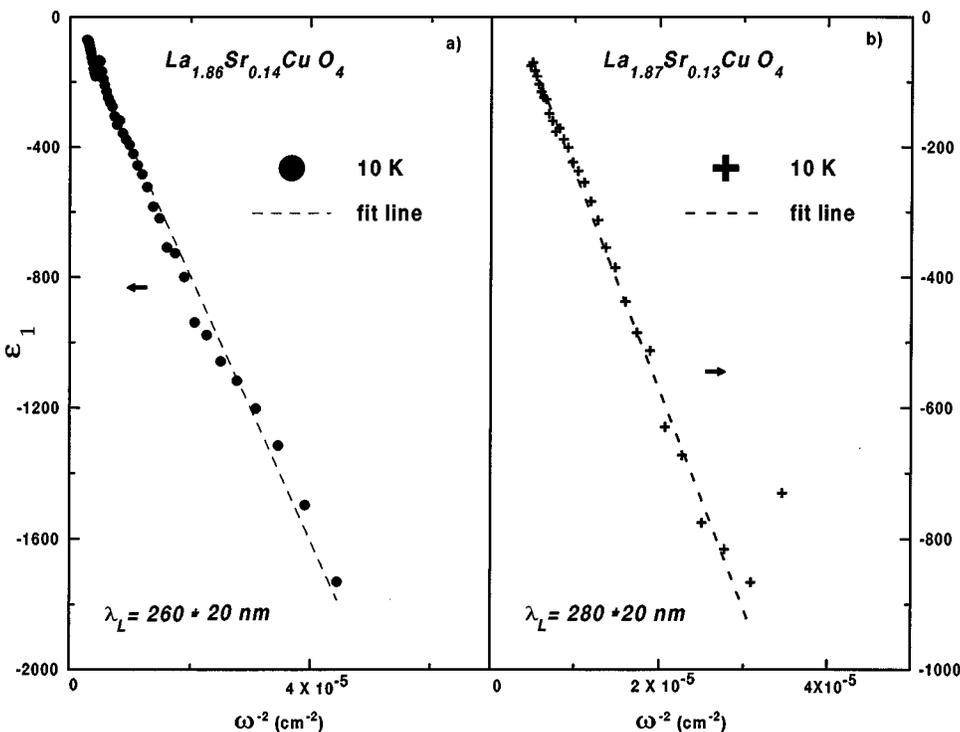

FIG. 3. The real part of the dielectric function as a function of ω^{-2} of $La_{1.86}Sr_{0.14}CuO_4$ at 10 K is shown in panel (a) and of $La_{1.87}Sr_{0.13}CuO_4$ at 25 K is shown in panel (b). The dash line is linear fit. The slope of the fit gives the values of the London penetration depth.
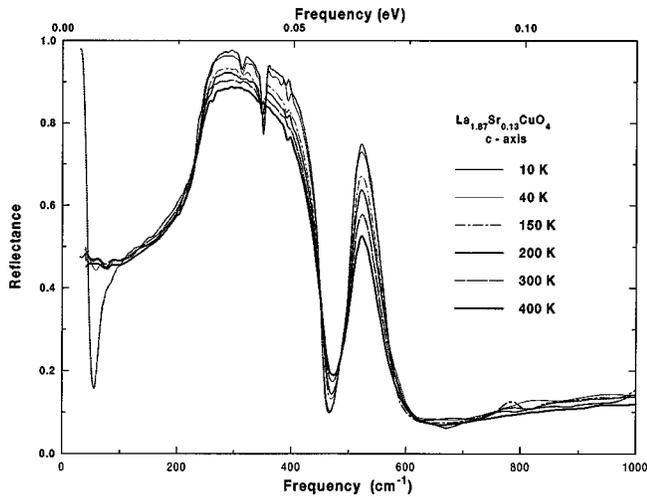
FIG. 4. The reflectance of $La_{1.87}Sr_{0.13}CuO_4$ with $E\|c$ axis is shown. The temperature sequences are 10, 40, 150, 200, 300, and 400 K.

The c-axis reflectance of the $x=0.13$ sample is shown in Fig. 4. The corresponding conductivity is low and is dominated by optical phonons (Fig. 5).

In YBCO 123 and 124 the pseudogap in c-axis conductivity manifests itself as a depression in conductivity at low frequency.[15,7,30] There is no coherent Drude peak and the conductivity is flat and frequency independent. In the temperature and doping range where a pseudogap is expected a low-frequency depression of conductivity is seen with an edge in the 300–400 cm^{-1} region where the conductivity rises to the high-frequency plateau.

In order to isolate the electronic features of our LSCO c-axis spectrum we magnify the low value region of σ_{1c} (Fig. 5). There is no sharp pseudogap edge in the low-
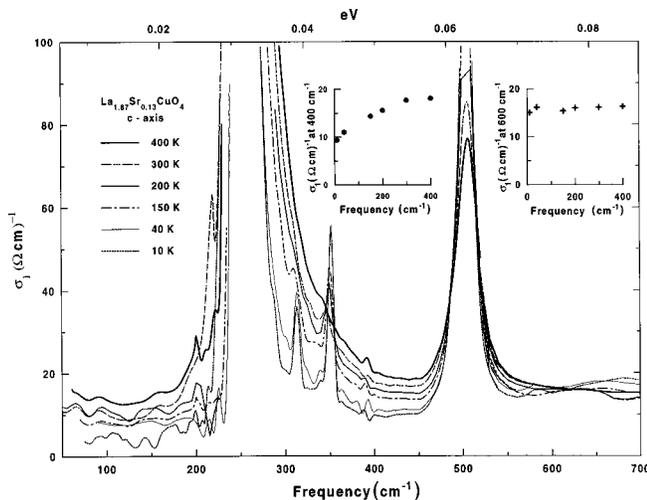

FIG. 5. The c-axis conductivity of the $La_{1.87}Sr_{0.13}CuO_4$ is shown at different temperatures. Since the phonon peaks are dominant in the direction perpendicular to CuO_2 planes, the graph is focused at the background conductivity. Two inserts are the c-axis conductivity of the underdoped $La_{1.87}Sr_{0.13}CuO_4$ measured at 450 and at 600 cm^{-1}. The c-axis conductivity at 450 cm^{-1} is depressed below 300 K, however, it is somewhat constant above 600 cm^{-1}. This could be a signature of the pseudogap formation at the temperatures less than 300 K and with the size of 500 cm^{-1}.

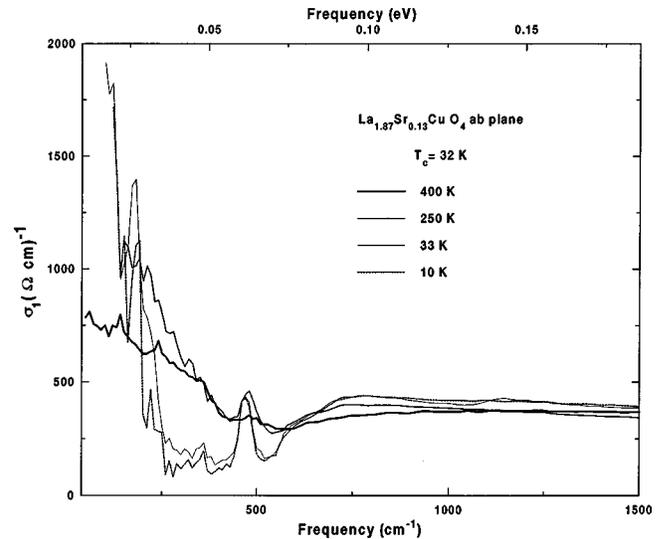FIG. 6. The ab-plane conductivity of the $La_{1.87}Sr_{0.13}CuO_4$ is shown at different temperatures.

frequency infrared data for underdoped LSCO as there is in the case of Y123. It is possible that such a feature could be hidden under the large phonon structure. Efforts to subtract the phonons in order to extract the background conductivity were found to be extremely sensitive to the choice of their shape in fitting procedures. Nonetheless, the raw data clearly show that there is low-frequency depression of the c-axis conductivity. Conductivity at 450 cm^{-1} is uniformly suppressed below $T=300$ K (Fig. 5, inset), whereas the conductivity at 600 cm^{-1} is nearly constant at all temperatures. Based on this analysis one can conclude that the pseudogap state in the c-axis opens up below 300 K and its size is approximately equal to 500 cm^{-1}.

Manifestations of the pseudogap in the ab-plane conductivity exist as a loss of spectral weight between 700 and 200 cm^{-1} balanced by increases both below and above this frequency. In both Figs. 6 and 7 one can see the temperature evolution of the sharp depression in ab conductivity below
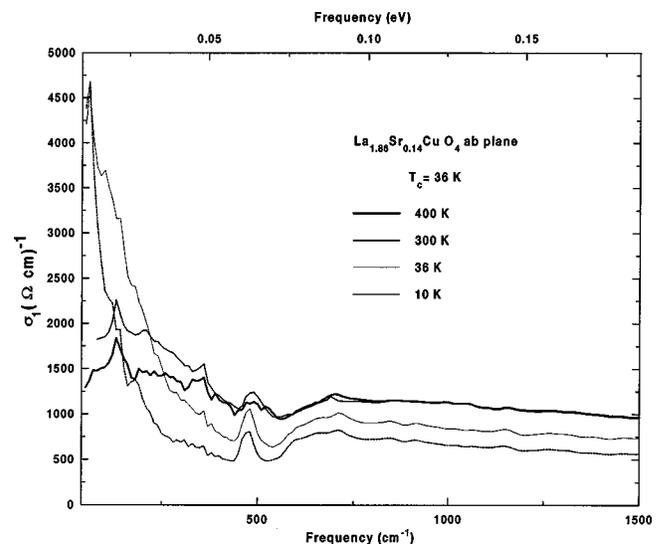

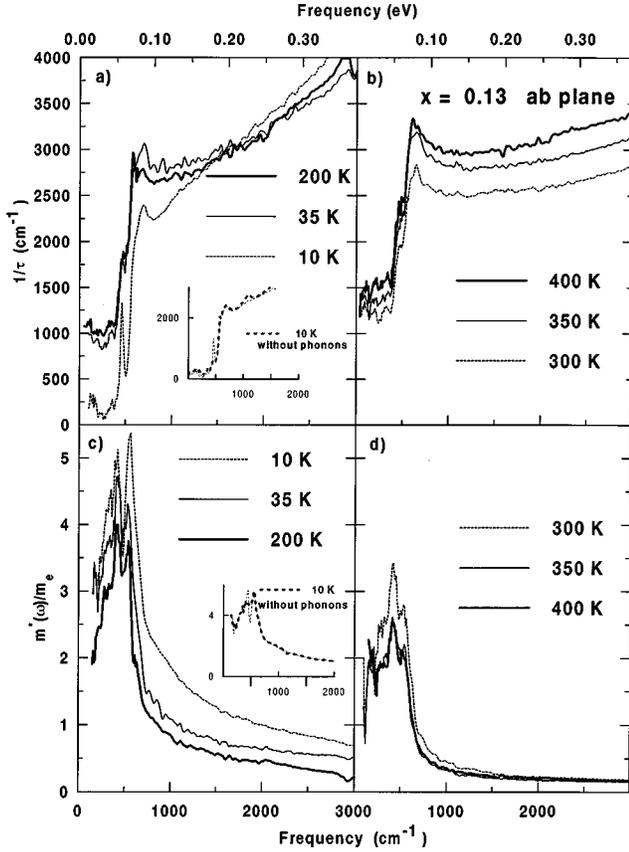FIG. 7. The ab-plane conductivity (a) of the $La_{1.86}Sr_{0.14}CuO_4$ is shown at different temperatures.

FIG. 8. Top panel: the low-temperature frequency-dependent scattering rate of $La_{1.87}Sr_{0.13}CuO_4$ below T^{**} (a) and above T^{**} (b) is calculated using Eq. (1). The onset of the suppression in a conductivity corresponds to a drastic change in the frequency dependence of the scattering rate below T^*. Above 700 cm^{-1} the scattering rate is nearly temperature independent and has a linear frequency dependence below T^{**}. Below 700 cm^{-1} the scattering rate varies as $\omega^{1+\delta}$ and shows a strong temperature dependence. Bottom panel: The effective mass of $La_{1.87}Sr_{0.13}CuO_4$ below T^{**} (a) and above T^{**} (b) is calculated using Eq. (2). The onset of enhancement of $m^*(\omega)/m_e$ corresponds to the onset of the suppression of the scattering rate.

700 cm^{-1} at temperatures above T_c. A much clearer picture of the pseudogap state can be seen from the effective scattering rate, $1/\tau(\omega,T)$, calculated from the conductivity using Eq. (1) which is shown along with the effective mass in Figs. 8 and 9. The $1/\tau(\omega,T)$ spectra can conveniently be divided into two regions. In the high-frequency region, starting at about 700 cm^{-1}, the scattering rate varies linearly with frequency while in the low-frequency region there is a clear suppression of $1/\tau(\omega,T)$ below this linear trend.[31] The temperature where this suppression first appears serves as a definition of T^*, the onset temperature of the pseudogap state. As the temperature is lowered below T^* this suppression becomes deeper. We find that for underdoped $La_{2-x}Sr_xCuO_4$ $T^* \geqslant 400$ K, an order of magnitude higher than the superconducting transition temperature T_c (32 K). This is significantly different from previous results on cuprates where T^* more or less coincides with T_c near optimal doping.

The temperature dependence above 700 cm^{-1} is strongly influenced by the level of Sr doping. In the underdoped sample the high-frequency scattering rate is nearly tempera-
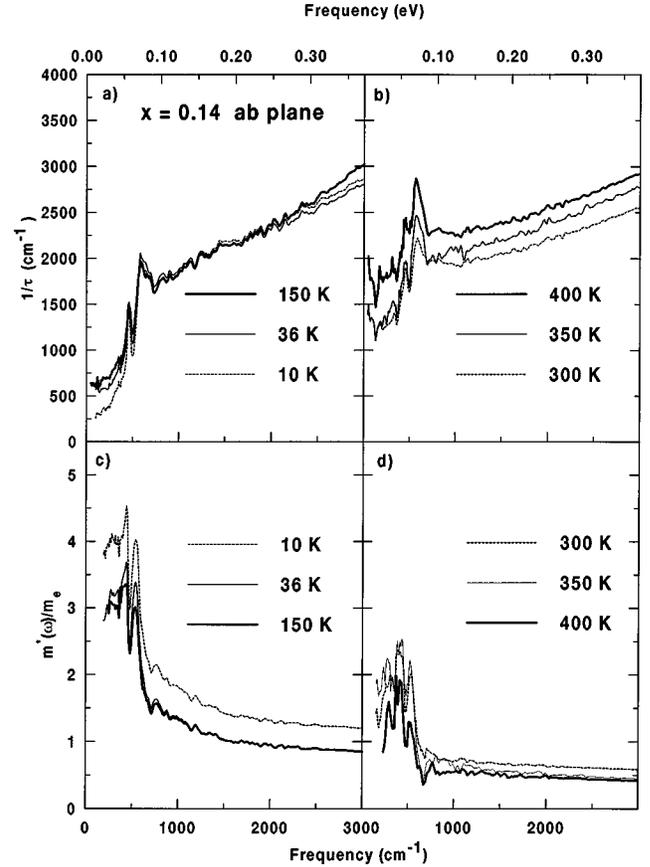
FIG. 9. Top panel: the high-temperature effective scattering rate of $La_{1.86}Sr_{0.14}CuO_4$ below T^{**} (a) and above T^{**} (b) is calculated using Eq. (1). Above 700 cm^{-1} the scattering rate has a linear frequency and temperature-independent below T^{**} (a) and temperature dependent above T^{**} (b). Below 700 cm^{-1} the scattering rate varies as $\omega^{1+\delta}$ and shows a strong temperature dependence. Bottom panel: The effective mass of $La_{1.87}Sr_{0.13}CuO_4$ below T^{**} (a) and above T^{**} (b) samples is calculated using Eq. (2).

ture independent up to a certain temperature [Figs. 8(a) and 9(a)], which we will call T^{**} above which a pronounced temperature dependence of $1/\tau(\omega,T)$ is seen [Figs. 8(b) and 9(b)]. In the $x=0.13$ sample $T^{**} \approx 200$ K, while in the $x=0.14$ sample $T^{**} \approx 150$ K. In the overdoped samples the scattering rate above 700 cm^{-1} increases uniformly with temperature[32] at all temperatures suggesting $T^{**} \to 0$ in that limit. This behavior is also seen in other overdoped HTSC's.[31]

If one extrapolates the 300 K scattering rates to zero frequency one finds that for the $x=0.13$ sample the scattering rate $1/\tau_0 \approx 2500$ cm^{-1} and for the $x=0.13$ sample this rate is ≈ 1500 cm^{-1}. These scattering rates are much higher than what is seen for the higher T_c materials reviewed by Puchkov *et al.*[31] where at 300 K $1/\tau_0 \approx 1000 \pm 200$ cm^{-1} for several families and many doping levels. This high residual scattering differentiates the LSCO material from the other cuprates.

If we call the frequency below which the scattering rate is suppressed the *ab*-plane pseudogap $\omega_{ab} \approx 700$ cm^{-1} we find it is clearly bigger than the *c*-axis pseudogap frequency $\omega_c \approx 500$ cm^{-1}.

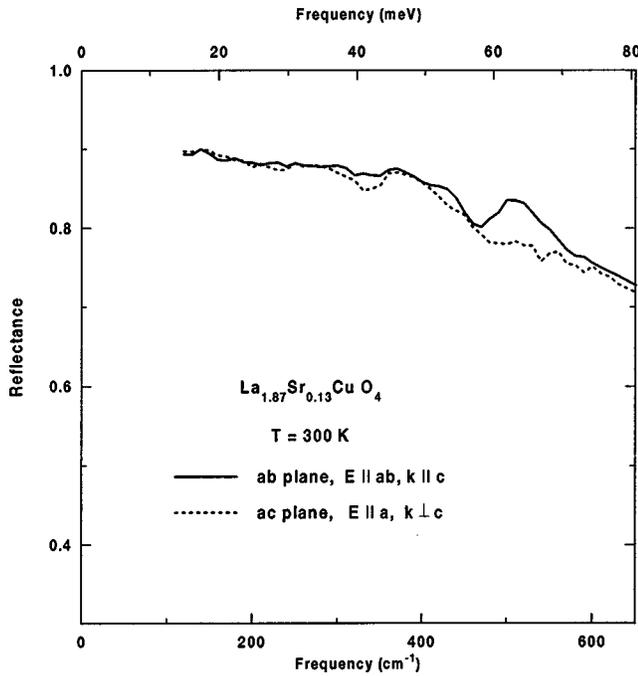In addition to the pseudogap depth and temperature dependence, several other features of Figs. 9 and 10 should be

FIG. 10. Comparison of the reflectance of $La_{1.87}Sr_{0.13}CuO_4$ measured from the ab-plane with $k\|c$ and from ac plane with $k\perp c$.

mentioned. The position of the pseudogap remains at 700 cm^{-1} for all temperatures. There are also several peaks positioned at 500 cm^{-1} in the scattering rate which complicate the analysis, particularly in the case of the sample with $x=0.14$. These peaks have been observed by other groups and have been attributed to polaronic effects.[33,34] Another possible explanation is the correlation of the ab-plane conductivity with c-axis LO phonons. We did observe the difference in contribution of LO phonons to the ab-plane reflectance with different propagation directions, an effect observed by Reedyk et al.,[35] and also seen in the $k\|c$ vs. $k\perp c$ spectra obtained by Tanner's group.[18] In Fig. 10 the reflectance with $E\|a$ and $k\|c$, is compared with the reflectance with $E\|ab$ and $k\|a$, with the $La_{1.87}Sr_{0.13}CuO_4$ sample at room temperature. There is an extra feature observed at 500 cm^{-1} in the spectra with $k\|c$. Further evidence that the c-axis LO phonons couples to ab-plane features can be seen in Fig. 11. The comparison between peaks in the effective scattering rate at 450 and 580 cm^{-1} to the peaks in Im$(-1/\epsilon_c)$ shows the same strong correlation seen in many other cuprates.[35]

For completeness we also plot the effective mass of underdoped samples at low temperatures [Fig. 8(c)] and high temperatures [Figs. 9(c) and 9(d)]. As expected, $m^*(\omega)/m_e$ rises to a maximum ≈ 3 forming a peak at ≈ 400 cm^{-1}. The enhancement of the effective mass in the pseudogap state as well as the upper limit of $m^*(\omega)/m_e$ are similar to what has been previously reported for Y123, Y124, and Bi2212.[31]

Before closing we compare our results with data of Gao et al.[19] on $La_{2-x}Sr_xCuO_{4+\delta}$ films and Quijada et al.[18] on oxygen-doped $La_2CuO_{4+\delta}$. Our results in the underdoped case are comparable with those of the oxygen-doped material, although Quijada et al. did not carry out a frequency-dependent scattering rate analysis for their underdoped sample. The film results of Gao et al. are quite different from
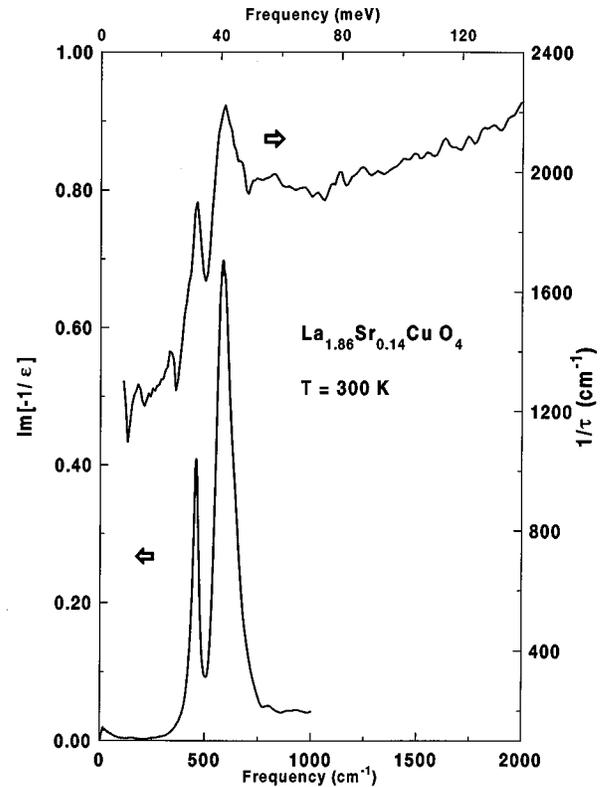

FIG. 11. Comparison of the peaks position at 450 and 580 cm^{-1} in the dielectric loss function of the c-axis phonons with the effective scattering rate of $La_{1.86}Sr_{0.14}CuO_4$ at room temperature. The correspondence of the peaks positions, width and the relative strength suggests that the nature of the peak may lie in the coupling of an ab-plane spectra to the c-axis longitudinal optical phonons.

our findings. The films used in that study had a strontium level that would correspond to optimal doping in crystals. However, the $1/\tau(\omega)$ curves deviate markedly from what we observe for slightly under and overdoped samples. The authors performed an extended Drude analysis and found a strongly temperature-dependent scattering rate even at low temperatures. This is in sharp contrast to our results which would suggest a very weak temperature dependence in this temperature region. Based on our work, their samples should be in the pseudogap state since they have an x value near optimal doping. Comparing these results with other systems, in particular with Tl2202, two factors suggest the possibility that the films may be overdoped. First, their T_c was near 30 K, lower than that expected for optimal doping. Secondly, it is known that the oxygen level in films can vary substantially and in LSCO oxygen can have a major influence on the doping level.[36] On the other hand, we cannot completely rule out the possibility that all the crystal results are affected by the polishing process, and that the films better represent the bulk material. It is clearly important to measure films where the oxygen content is controlled by selective annealing.

In conclusion, the optical data in the far-infrared region, taken on two underdoped single-layered high-T_c superconductors, shows clear evidence of a pseudogap state in both the scattering rate and conductivity along CuO$_2$ planes. This pseudogap state extends to higher temperatures than that ob-

served in the multilayered underdoped cuprates such as YBCO and BSCO.

The scattering rate is similar for both systems in the pseudogap state. At low frequencies, $\omega \lesssim 700$ cm^{-1}, the scattering rates are *temperature* dependent and change with frequency in a *nonlinear* fashion. Above 700 cm^{-1} this behavior becomes *linear*. Within experimental uncertainty the observed high-frequency scattering rate of the underdoped sample is *not affected by temperature* up to certain temperature T^{**}. This temperature is equal to 200 K in case of $La_{1.87}Sr_{0.13}CuO_4$ and 150 K in case of $La_{1.86}Sr_{0.14}CuO_4$. Above T^{**} the high-frequency scattering rate is temperature dependent. This behavior is identical to the high-frequency effective scattering rate of an overdoped HTSC.[31]

Our findings in the direction perpendicular to the CuO_2 planes showed that the depression of the *c*-axis conductivity is not as prominent as the one found in the two-layer HTSC. Nevertheless, the signature of the pseudogap can be seen at the frequencies below 500 cm^{-1} up to room temperature.

[1] T. Timusk and B. Statt, Rep. Prog. Phys. (to be published).

[2] D. S. Marshall, A. G. Loeser, Z.-X. Chen, and D. S. Dessau, Physica C **263**, 208 (1999).

[3] H. J. Tao, F. Lu, and E. L. Wolf, Physica B & C **282-287C**, 1507 (1987); Ch. Renner, B. Revaz, J.-Y. Genoud, K. Kadowaki, and O. Fischer, Phys. Rev. Lett. **80**, 149 (1998).

[4] B. Bucher, P. Steiner, J. Karpinski, E. Kaldis, and P. Wachter, Phys. Rev. Lett. **70**, 2012 (1993).

[5] T. Ito, K. Takenaka, and S. Uchida, Phys. Rev. Lett. **70**, 3995 (1993).

[6] B. Batlogg, H. Y. Hwang, H. Takagi, R. J. Cava, H. L. Kao, and J. Kuo, Physica C **235-240**, 130 (1994).

[7] D. N. Basov, R. Liang, B. Dabrowski, D. A. Bonn, W. N. Hardy, and T. Timusk, Phys. Rev. Lett. **77**, 4090 (1996).

[8] A. V. Puchkov, P. Fournier, D. N. Basov, T. Timusk, A. Kapitulnik, and N. N. Kolesnikov, Phys. Rev. Lett. **77**, 3212 (1996).

[9] A. V. Puchkov, P. Fournier, T. Timusk, and N. N. Kolesnikov, Phys. Rev. Lett. **77**, 1853 (1996).

[10] A. J. Millis and H. Monien, Phys. Rev. Lett. **70**, 2810 (1993).

[11] T. E. Mason, G. Aeppli, and H. A. Mook, Phys. Rev. Lett. **68**, 1414 (1992).

[12] S. Uchida, T. Ido, H. Takagi, T. Arima, Y. Tokura, and S. Tajima, Phys. Rev. B **43**, 7942 (1991).

[13] H. Y. Hwang, B. Batlogg, H. Takagi, H. L. Kao, J. Kwo, R. J. Cava, J. J. Krajewski, and W. F. Peck, Phys. Rev. Lett. **72**, 2636 (1994).

[14] S. K. Tolpygo, J.-Y. Lin, M. Gurvitch, S. Y. Hou, and Julia M. Phillips, Phys. Rev. B **53**, 12 454 (1996).

[15] C. C. Homes, T. Timusk, R. Liang, D. A. Bonn, and W. N. Hardy, Phys. Rev. Lett. **71**, 1645 (1993).

[16] D. N. Basov, H. A. Mook, B. Dabrowski, and T. Timusk, Phys. Rev. B **52**, R13 141 (1995).

[17] S. Uchida, K. Tamasaku, and S. Tajima, Phys. Rev. B **53**, 14 558 (1996).

[18] M. A. Quijada, D. B. Tanner, F. C. Chou, D. C. Johnston, and S.-W. Cheong, Phys. Rev. B **52**, 15 485 (1995).

[19] F. Gao, D. B. Romero, B. D. Tanner, J. Talvacchio, and M. G. Forrester, Phys. Rev. B **47**, 1036 (1993).

[20] W. Götze and P. Wolfle, Phys. Rev. B **6**, 1226 (1972).

[21] P. B. Allen, Phys. Rev. B **3**, 305 (1971).

[22] A. Gold, S. J. Allen, B. A. Wilson, and D. C. Tsui, Phys. Rev. B **25**, 3519 (1982).

[23] S.-W. Cheong, G. Aeppli, T. E. Mason, H. Mook, S. M. Hayden, P. C. Canfield, Z. Fisk, K. N. Clausen, and J. L. Martinez, Phys. Rev. Lett. **67**, 1791 (1991).

[24] T. Kimura, K. Kishio, T. Kobayashi, Y. Nakayama, N. Motohira, K. Kitazawa, and K. Yamafuji, Physica C **192**, 247 (1992).

[25] J. Orenstein and D. H. Rapkine, Phys. Rev. Lett. **60**, 968 (1988).

[26] S. Tajima, S. Uchida, S. Ishibashi, T. Ido, H. Takagi, T. Arima, and Y. Tokura, Physica C **168**, 117 (1990).

[27] H. Takagi, B. Batlogg, H. L. Kao, J. Kwo, R. J. Cava, J. J. Krajewski, and W. F. Peck, Jr., Phys. Rev. Lett. **69**, 2975 (1992).

[28] D. B. Tanner and T. Timusk, in *Physical Properties of High Temperature Superconductors I*, edited by D. M. Ginsberg (World Scientific, Singapore, 1992), p. 363.

[29] G. Aeppli, R. J. Cava, E. J. Ansaldo, J. H. Brewer, S. R. Kreitzman, G. M. Luke, D. R. Noakes, and R. F. Kiefl, Phys. Rev. B **35**, 7129 (1987).

[30] C. C. Homes, T. Timusk, R. Liang, D. A. Bonn, and W. H. Hardy, Physica C **254**, 265-280 (1995).

[31] A. V. Puchkov, D. N. Basov, and T. Timusk, J. Phys.: Condens. Matter **8**, 10 049 (1996).

[32] T. Startseva, T. Timusk, M. Okuya, T. Kimura, and K. Kishio (unpublished).

[33] Y. Yagil and E. K. H. Salje, Physica C **235-140**, 1143 (1994).

[34] G. A. Thomas, D. H. Rapkine, S. L. Cooper, S.-W. Cheong, A. S. Cooper, L. S. Schneemeyer, and J. V. Waszczak, Phys. Rev. B **45**, 2474 (1992).

[35] M. Reedyk and T. Timusk, Phys. Rev. Lett. **69**, 2705 (1992).

[36] H. Zhang, H. Sato, and G. L. Liedl, Physica C **234**, 185 (1994).